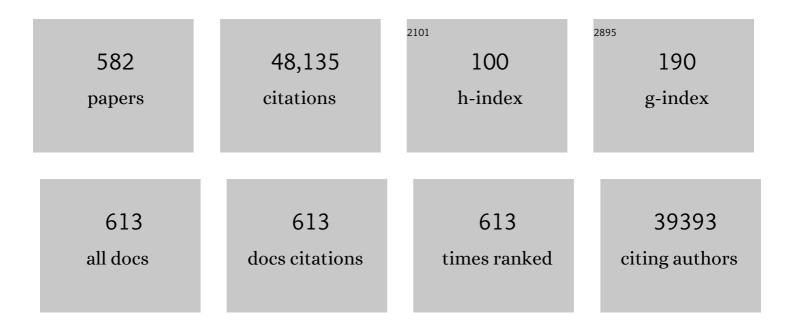
Daniel Rueckert

List of Publications by Year in descending order

Source: https://exaly.com/author-pdf/5116447/publications.pdf Version: 2024-02-01



#	Article	IF	CITATIONS
1	Tract-based spatial statistics: Voxelwise analysis of multi-subject diffusion data. NeuroImage, 2006, 31, 1487-1505.	4.2	5,755
2	Real-Time Single Image and Video Super-Resolution Using an Efficient Sub-Pixel Convolutional Neural Network. , 2016, , .		3,557
3	Efficient multi-scale 3D CNN with fully connected CRF for accurate brain lesion segmentation. Medical Image Analysis, 2017, 36, 61-78.	11.6	2,382
4	Evaluation of 14 nonlinear deformation algorithms applied to human brain MRI registration. NeuroImage, 2009, 46, 786-802.	4.2	1,988
5	Attention gated networks: Learning to leverage salient regions in medical images. Medical Image Analysis, 2019, 53, 197-207.	11.6	1,011
6	A Deep Cascade of Convolutional Neural Networks for Dynamic MR Image Reconstruction. IEEE Transactions on Medical Imaging, 2018, 37, 491-503.	8.9	816
7	Multi-atlas based segmentation of brain images: Atlas selection and its effect on accuracy. NeuroImage, 2009, 46, 726-738.	4.2	797
8	Automatic anatomical brain MRI segmentation combining label propagation and decision fusion. NeuroImage, 2006, 33, 115-126.	4.2	794
9	Acquisition and voxelwise analysis of multi-subject diffusion data with Tract-Based Spatial Statistics. Nature Protocols, 2007, 2, 499-503.	12.0	526
10	Anatomically Constrained Neural Networks (ACNNs): Application to Cardiac Image Enhancement and Segmentation. IEEE Transactions on Medical Imaging, 2018, 37, 384-395.	8.9	493
11	Secure, privacy-preserving and federated machine learning in medical imaging. Nature Machine Intelligence, 2020, 2, 305-311.	16.0	473
12	Automated cardiovascular magnetic resonance image analysis with fully convolutional networks. Journal of Cardiovascular Magnetic Resonance, 2018, 20, 65.	3.3	468
13	Deep Learning for Cardiac Image Segmentation: A Review. Frontiers in Cardiovascular Medicine, 2020, 7, 25.	2.4	467
14	Disease prediction using graph convolutional networks: Application to Autism Spectrum Disorder and Alzheimer's disease. Medical Image Analysis, 2018, 48, 117-130.	11.6	391
15	Random forest-based similarity measures for multi-modal classification of Alzheimer's disease. NeuroImage, 2013, 65, 167-175.	4.2	376
16	Convolutional Recurrent Neural Networks for Dynamic MR Image Reconstruction. IEEE Transactions on Medical Imaging, 2019, 38, 280-290.	8.9	362
17	ISLES 2015 - A public evaluation benchmark for ischemic stroke lesion segmentation from multispectral MRI. Medical Image Analysis, 2017, 35, 250-269.	11.6	360
18	Fast and robust multi-atlas segmentation of brain magnetic resonance images. Neurolmage, 2010, 49, 2352-2365.	4.2	357

#	Article	IF	CITATIONS
19	Automatic construction of 3-D statistical deformation models of the brain using nonrigid registration. IEEE Transactions on Medical Imaging, 2003, 22, 1014-1025.	8.9	350
20	A Review of Deep Learning in Medical Imaging: Imaging Traits, Technology Trends, Case Studies With Progress Highlights, and Future Promises. Proceedings of the IEEE, 2021, 109, 820-838.	21.3	339
21	Automatic construction of multiple-object three-dimensional statistical shape models: application to cardiac modeling. IEEE Transactions on Medical Imaging, 2002, 21, 1151-1166.	8.9	325
22	The developing human connectome project: A minimal processing pipeline for neonatal cortical surface reconstruction. Neurolmage, 2018, 173, 88-112.	4.2	315
23	Self-supervised learning for medical image analysis using image context restoration. Medical Image Analysis, 2019, 58, 101539.	11.6	315
24	Case-mix, care pathways, and outcomes in patients with traumatic brain injury in CENTER-TBI: a European prospective, multicentre, longitudinal, cohort study. Lancet Neurology, The, 2019, 18, 923-934.	10.2	304
25	Automatic segmentation of brain MRIs of 2-year-olds into 83 regions of interest. NeuroImage, 2008, 40, 672-684.	4.2	301
26	Rich-club organization of the newborn human brain. Proceedings of the National Academy of Sciences of the United States of America, 2014, 111, 7456-7461.	7.1	300
27	Automatic Whole Brain MRI Segmentation of the Developing Neonatal Brain. IEEE Transactions on Medical Imaging, 2014, 33, 1818-1831.	8.9	296
28	Human brain mapping: A systematic comparison of parcellation methods for the human cerebral cortex. NeuroImage, 2018, 170, 5-30.	4.2	280
29	Geodesic Information Flows: Spatially-Variant Graphs and Their Application to Segmentation and Fusion. IEEE Transactions on Medical Imaging, 2015, 34, 1976-1988.	8.9	265
30	The Effect of Preterm Birth on Thalamic and Cortical Development. Cerebral Cortex, 2012, 22, 1016-1024.	2.9	262
31	DeepCut: Object Segmentation From Bounding Box Annotations Using Convolutional Neural Networks. IEEE Transactions on Medical Imaging, 2017, 36, 674-683.	8.9	260
32	Construction of a consistent high-definition spatio-temporal atlas of the developing brain using adaptive kernel regression. NeuroImage, 2012, 59, 2255-2265.	4.2	259
33	Titin-truncating variants affect heart function in disease cohorts and the general population. Nature Genetics, 2017, 49, 46-53.	21.4	255
34	Segmentation of 4D cardiac MR images using a probabilistic atlas and the EM algorithm. Medical Image Analysis, 2004, 8, 255-265.	11.6	249
35	A dynamic 4D probabilistic atlas of the developing brain. NeuroImage, 2011, 54, 2750-2763.	4.2	247
36	SonoNet: Real-Time Detection and Localisation of Fetal Standard Scan Planes in Freehand Ultrasound. IEEE Transactions on Medical Imaging, 2017, 36, 2204-2215.	8.9	246

#	Article	IF	CITATIONS
37	Unsupervised Domain Adaptation in Brain Lesion Segmentation with Adversarial Networks. Lecture Notes in Computer Science, 2017, , 597-609.	1.3	241
38	Multi-Method Analysis of MRI Images in Early Diagnostics of Alzheimer's Disease. PLoS ONE, 2011, 6, e25446.	2.5	240
39	Metric learning with spectral graph convolutions on brain connectivity networks. NeuroImage, 2018, 169, 431-442.	4.2	237
40	Automated Abdominal Multi-Organ Segmentation With Subject-Specific Atlas Generation. IEEE Transactions on Medical Imaging, 2013, 32, 1723-1730.	8.9	225
41	Fully automatic acute ischemic lesion segmentation in DWI using convolutional neural networks. NeuroImage: Clinical, 2017, 15, 633-643.	2.7	221
42	Abnormal deep grey matter development following preterm birth detected using deformation-based morphometry. NeuroImage, 2006, 32, 70-78.	4.2	220
43	Multimodal surface matching with higher-order smoothness constraints. NeuroImage, 2018, 167, 453-465.	4.2	219
44	LEAP: Learning embeddings for atlas propagation. NeuroImage, 2010, 49, 1316-1325.	4.2	216
45	Semi-supervised Learning for Network-Based Cardiac MR Image Segmentation. Lecture Notes in Computer Science, 2017, , 253-260.	1.3	209
46	The influence of preterm birth on the developing thalamocortical connectome. Cortex, 2013, 49, 1711-1721.	2.4	202
47	DRINet for Medical Image Segmentation. IEEE Transactions on Medical Imaging, 2018, 37, 2453-2462.	8.9	198
48	Segmentation of MR images via discriminative dictionary learning and sparse coding: Application to hippocampus labeling. NeuroImage, 2013, 76, 11-23.	4.2	196
49	Automatic segmentation and reconstruction of the cortex from neonatal MRI. NeuroImage, 2007, 38, 461-477.	4.2	192
50	Diffeomorphic Registration Using B-Splines. Lecture Notes in Computer Science, 2006, 9, 702-709.	1.3	190
51	Right ventricle segmentation from cardiac MRI: A collation study. Medical Image Analysis, 2015, 19, 187-202.	11.6	189
52	A Deep Cascade of Convolutional Neural Networks for MR Image Reconstruction. Lecture Notes in Computer Science, 2017, , 647-658.	1.3	187
53	A Generic Framework for Non-rigid Registration Based on Non-uniform Multi-level Free-Form Deformations. Lecture Notes in Computer Science, 2001, , 573-581.	1.3	185
54	An evaluation of four automatic methods of segmenting the subcortical structures in the brain. NeuroImage, 2009, 47, 1435-1447.	4.2	180

#	Article	IF	CITATIONS
55	Deep-learning cardiac motion analysis for human survival prediction. Nature Machine Intelligence, 2019, 1, 95-104.	16.0	179
56	Magnetic resonance imaging of the newborn brain: Manual segmentation of labelled atlases in term-born and preterm infants. NeuroImage, 2012, 62, 1499-1509.	4.2	175
57	Improving intersubject image registration using tissue-class information benefits robustness and accuracy of multi-atlas based anatomical segmentation. NeuroImage, 2010, 51, 221-227.	4.2	174
58	A Probabilistic Patch-Based Label Fusion Model for Multi-Atlas Segmentation With Registration Refinement: Application to Cardiac MR Images. IEEE Transactions on Medical Imaging, 2013, 32, 1302-1315.	8.9	174
59	MRI of Moving Subjects Using Multislice Snapshot Images With Volume Reconstruction (SVR): Application to Fetal, Neonatal, and Adult Brain Studies. IEEE Transactions on Medical Imaging, 2007, 26, 967-980.	8.9	173
60	Dictionary Learning and Time Sparsity for Dynamic MR Data Reconstruction. IEEE Transactions on Medical Imaging, 2014, 33, 979-994.	8.9	173
61	DeepMedic for Brain Tumor Segmentation. Lecture Notes in Computer Science, 2016, , 138-149.	1.3	170
62	Regional growth and atlasing of the developing human brain. NeuroImage, 2016, 125, 456-478.	4.2	167
63	Multi-modal classification of Alzheimer's disease using nonlinear graph fusion. Pattern Recognition, 2017, 63, 171-181.	8.1	166
64	Multiple instance learning for classification of dementia in brain MRI. Medical Image Analysis, 2014, 18, 808-818.	11.6	163
65	Machine Learning of Three-dimensional Right Ventricular Motion Enables Outcome Prediction in Pulmonary Hypertension: A Cardiac MR Imaging Study. Radiology, 2017, 283, 381-390.	7.3	161
66	Machine learning in cardiovascular magnetic resonance: basic concepts and applications. Journal of Cardiovascular Magnetic Resonance, 2019, 21, 61.	3.3	157
67	End-to-end privacy preserving deep learning on multi-institutional medical imaging. Nature Machine Intelligence, 2021, 3, 473-484.	16.0	157
68	Automatic 3D Bi-Ventricular Segmentation of Cardiac Images by a Shape-Refined Multi- Task Deep Learning Approach. IEEE Transactions on Medical Imaging, 2019, 38, 2151-2164.	8.9	155
69	An optimised tract-based spatial statistics protocol for neonates: Applications to prematurity and chronic lung disease. NeuroImage, 2010, 53, 94-102.	4.2	154
70	Cardiac Image Super-Resolution with Global Correspondence Using Multi-Atlas PatchMatch. Lecture Notes in Computer Science, 2013, 16, 9-16.	1.3	150
71	A global benchmark of algorithms for segmenting the left atrium from late gadolinium-enhanced cardiac magnetic resonance imaging. Medical Image Analysis, 2021, 67, 101832.	11.6	150
72	A common neonatal image phenotype predicts adverse neurodevelopmental outcome in children born preterm. NeuroImage, 2010, 52, 409-414.	4.2	147

#	Article	IF	CITATIONS
73	Diffeomorphic 3D Image Registration via Geodesic Shooting Using an Efficient Adjoint Calculation. International Journal of Computer Vision, 2012, 97, 229-241.	15.6	146
74	Robust whole-brain segmentation: Application to traumatic brain injury. Medical Image Analysis, 2015, 21, 40-58.	11.6	146
75	A review on automatic fetal and neonatal brain MRI segmentation. NeuroImage, 2018, 170, 231-248.	4.2	143
76	Benchmarking framework for myocardial tracking and deformation algorithms: An open access database. Medical Image Analysis, 2013, 17, 632-648.	11.6	140
77	Fast Volume Reconstruction From Motion Corrupted Stacks of 2D Slices. IEEE Transactions on Medical Imaging, 2015, 34, 1901-1913.	8.9	138
78	Multi-atlas segmentation with augmented features for cardiac MR images. Medical Image Analysis, 2015, 19, 98-109.	11.6	137
79	Differential diagnosis of neurodegenerative diseases using structural MRI data. NeuroImage: Clinical, 2016, 11, 435-449.	2.7	137
80	Multi-region analysis of longitudinal FDG-PET for the classification of Alzheimer's disease. NeuroImage, 2012, 60, 221-229.	4.2	136
81	Evaluation of current algorithms for segmentation of scar tissue from late Gadolinium enhancement cardiovascular magnetic resonance of the left atrium: an open-access grand challenge. Journal of Cardiovascular Magnetic Resonance, 2013, 15, 105.	3.3	136
82	Analysis of 3-D Myocardial Motion in Tagged MR Images Using Nonrigid Image Registration. IEEE Transactions on Medical Imaging, 2004, 23, 1245-1250.	8.9	135
83	Federated deep learning for detecting COVID-19 lung abnormalities in CT: a privacy-preserving multinational validation study. Npj Digital Medicine, 2021, 4, 60.	10.9	134
84	Prediction of stroke thrombolysis outcome using CT brain machine learning. Neurolmage: Clinical, 2014, 4, 635-640.	2.7	131
85	Injury markers predict time to dementia in subjects with MCI and amyloid pathology. Neurology, 2012, 79, 1809-1816.	1.1	129
86	Automated processing pipeline for neonatal diffusion MRI in the developing Human Connectome Project. Neurolmage, 2019, 185, 750-763.	4.2	127
87	Measurement of hippocampal atrophy using 4D graph-cut segmentation: Application to ADNI. NeuroImage, 2010, 52, 109-118.	4.2	122
88	Discriminative dictionary learning for abdominal multi-organ segmentation. Medical Image Analysis, 2015, 23, 92-104.	11.6	122
89	CINENet: deep learning-based 3D cardiac CINE MRI reconstruction with multi-coil complex-valued 4D spatio-temporal convolutions. Scientific Reports, 2020, 10, 13710.	3.3	122
90	Spatio-temporal free-form registration of cardiac MR image sequences. Medical Image Analysis, 2005, 9, 441-456.	11.6	121

#	Article	IF	CITATIONS
91	Sparse reduced-rank regression detects genetic associations with voxel-wise longitudinal phenotypes in Alzheimer's disease. NeuroImage, 2012, 60, 700-716.	4.2	121
92	Evaluating reinforcement learning agents for anatomical landmark detection. Medical Image Analysis, 2019, 53, 156-164.	11.6	121
93	Automatic morphometry in Alzheimer's disease and mild cognitive impairment. NeuroImage, 2011, 56, 2024-2037.	4.2	120
94	Automated analysis of atrial late gadolinium enhancement imaging that correlates with endocardial voltage and clinical outcomes: A 2-center study. Heart Rhythm, 2013, 10, 1184-1191.	0.7	120
95	A Novel Grading Biomarker for the Prediction of Conversion From Mild Cognitive Impairment to Alzheimer's Disease. IEEE Transactions on Biomedical Engineering, 2017, 64, 155-165.	4.2	120
96	A bi-ventricular cardiac atlas built from 1000+ high resolution MR images of healthy subjects and an analysis of shape and motion. Medical Image Analysis, 2015, 26, 133-145.	11.6	119
97	Multi-input Cardiac Image Super-Resolution Using Convolutional Neural Networks. Lecture Notes in Computer Science, 2016, , 246-254.	1.3	119
98	Automatic quantification of normal cortical folding patterns from fetal brain MRI. NeuroImage, 2014, 91, 21-32.	4.2	118
99	Clobal Burden of Small Vessel Disease–Related Brain Changes on MRI Predicts Cognitive and Functional Decline. Stroke, 2020, 51, 170-178.	2.0	115
100	Registration and tracking to integrate X-ray and MR images in an XMR facility. IEEE Transactions on Medical Imaging, 2003, 22, 1369-1378.	8.9	111
101	Evaluation of Six Registration Methods for the Human Abdomen on Clinically Acquired CT. IEEE Transactions on Biomedical Engineering, 2016, 63, 1563-1572.	4.2	111
102	Fast generation of digitally reconstructed radiographs using attenuation fields with application to 2D-3D image registration. IEEE Transactions on Medical Imaging, 2005, 24, 1441-1454.	8.9	110
103	Fast and robust extraction of hippocampus from MR images for diagnostics of Alzheimer's disease. NeuroImage, 2011, 56, 185-196.	4.2	109
104	Structural brain imaging in Alzheimer's disease and mild cognitive impairment: biomarker analysis and shared morphometry database. Scientific Reports, 2018, 8, 11258.	3.3	106
105	Spectral Graph Convolutions for Population-Based Disease Prediction. Lecture Notes in Computer Science, 2017, , 177-185.	1.3	104
106	Comparison and Evaluation of Rigid, Affine, and Nonrigid Registration of Breast MR Images. Journal of Computer Assisted Tomography, 1999, 23, 800-805.	0.9	103
107	A population-based phenome-wide association study of cardiac and aortic structure and function. Nature Medicine, 2020, 26, 1654-1662.	30.7	98
108	Longitudinal regional brain volume changes quantified in normal aging and Alzheimer's APP×PS1 mice using MRI. Brain Research, 2009, 1270, 19-32.	2.2	97

#	Article	IF	CITATIONS
109	Dynamic patterns of cortical expansion during folding of the preterm human brain. Proceedings of the National Academy of Sciences of the United States of America, 2018, 115, 3156-3161.	7.1	94
110	Automatic detection and quantification of hippocampal atrophy on MRI in temporal lobe epilepsy: A proof-of-principle study. NeuroImage, 2007, 36, 38-47.	4.2	91
111	Recognition of 3D facial expression dynamics. Image and Vision Computing, 2012, 30, 762-773.	4.5	91
112	The estimation of patient-specific cardiac diastolic functions from clinical measurements. Medical Image Analysis, 2013, 17, 133-146.	11.6	91
113	Early growth in brain volume is preserved in the majority of preterm infants. Annals of Neurology, 2007, 62, 185-192.	5.3	89
114	Diffusion tensor imaging (DTI) of the brain in moving subjects: Application to inâ€utero fetal and exâ€utero studies. Magnetic Resonance in Medicine, 2009, 62, 645-655.	3.0	88
115	Multi-template tensor-based morphometry: Application to analysis of Alzheimer's disease. NeuroImage, 2011, 56, 1134-1144.	4.2	88
116	Registration-Based Interpolation. IEEE Transactions on Medical Imaging, 2004, 23, 922-926.	8.9	87
117	Identifying population differences in whole-brain structural networks: A machine learning approach. NeuroImage, 2010, 50, 910-919.	4.2	86
118	Measurements of medial temporal lobe atrophy for prediction of Alzheimer's disease in subjects with mild cognitive impairment. Neurobiology of Aging, 2013, 34, 2003-2013.	3.1	86
119	Genetic and functional insights into the fractal structure of the heart. Nature, 2020, 584, 589-594.	27.8	86
120	Evaluation of automatic neonatal brain segmentation algorithms: The NeoBrainS12 challenge. Medical Image Analysis, 2015, 20, 135-151.	11.6	85
121	Reverse Classification Accuracy: Predicting Segmentation Performance in the Absence of Ground Truth. IEEE Transactions on Medical Imaging, 2017, 36, 1597-1606.	8.9	85
122	Construction of a neonatal cortical surface atlas using Multimodal Surface Matching in the Developing Human Connectome Project. NeuroImage, 2018, 179, 11-29.	4.2	83
123	Multiclass semantic segmentation and quantification of traumatic brain injury lesions on head CT using deep learning: an algorithm development and multicentre validation study. The Lancet Digital Health, 2020, 2, e314-e322.	12.3	83
124	Self-supervision with Superpixels: Training Few-Shot Medical Image Segmentation Without Annotation. Lecture Notes in Computer Science, 2020, , 762-780.	1.3	83
125	Standardized Evaluation System for Left Ventricular Segmentation Algorithms in 3D Echocardiography. IEEE Transactions on Medical Imaging, 2016, 35, 967-977.	8.9	82
126	The developing Human Connectome Project (dHCP) automated resting-state functional processing framework for newborn infants. NeuroImage, 2020, 223, 117303.	4.2	81

#	Article	IF	CITATIONS
127	Magnetic Resonance Imaging of the Newborn Brain: Automatic Segmentation of Brain Images into 50 Anatomical Regions. PLoS ONE, 2013, 8, e59990.	2.5	78
128	Automated quality control in image segmentation: application to the UK Biobank cardiovascular magnetic resonance imaging study. Journal of Cardiovascular Magnetic Resonance, 2019, 21, 18.	3.3	78
129	Self-Supervised Learning for Cardiac MR Image Segmentation by Anatomical Position Prediction. Lecture Notes in Computer Science, 2019, , 541-549.	1.3	78
130	Simultaneous Multi-scale Registration Using Large Deformation Diffeomorphic Metric Mapping. IEEE Transactions on Medical Imaging, 2011, 30, 1746-1759.	8.9	75
131	Test sequence of CSF and MRI biomarkers for prediction of AD in subjects with MCI. Neurobiology of Aging, 2012, 33, 2272-2281.	3.1	75
132	A Multicenter, Scan-Rescan, Human and Machine Learning CMR Study to Test Generalizability and Precision in Imaging Biomarker Analysis. Circulation: Cardiovascular Imaging, 2019, 12, e009214.	2.6	75
133	The Developing Human Connectome Project: typical and disrupted perinatal functional connectivity. Brain, 2021, 144, 2199-2213.	7.6	75
134	A Comprehensive Cardiac Motion Estimation Framework Using Both Untagged and 3-D Tagged MR Images Based on Nonrigid Registration. IEEE Transactions on Medical Imaging, 2012, 31, 1263-1275.	8.9	74
135	Automated fetal brain segmentation from 2D MRI slices for motion correction. NeuroImage, 2014, 101, 633-643.	4.2	74
136	Joint Learning of Motion Estimation and Segmentation for Cardiac MR Image Sequences. Lecture Notes in Computer Science, 2018, , 472-480.	1.3	74
137	Improving the Generalizability of Convolutional Neural Network-Based Segmentation on CMR Images. Frontiers in Cardiovascular Medicine, 2020, 7, 105.	2.4	74
138	Automatic CNN-based detection of cardiac MR motion artefacts using k-space data augmentation and curriculum learning. Medical Image Analysis, 2019, 55, 136-147.	11.6	71
139	Multi-atlas pancreas segmentation: Atlas selection based on vessel structure. Medical Image Analysis, 2017, 39, 18-28.	11.6	70
140	Recurrent Neural Networks for Aortic Image Sequence Segmentation with Sparse Annotations. Lecture Notes in Computer Science, 2018, , 586-594.	1.3	69
141	Multiatlas whole heart segmentation of CT data using conditional entropy for atlas ranking and selection. Medical Physics, 2015, 42, 3822-3833.	3.0	66
142	Multi-organ Segmentation Based on Spatially-Divided Probabilistic Atlas from 3D Abdominal CT Images. Lecture Notes in Computer Science, 2013, 16, 165-172.	1.3	62
143	Statistical Shape Modeling of the Left Ventricle: Myocardial Infarct Classification Challenge. IEEE Journal of Biomedical and Health Informatics, 2018, 22, 503-515.	6.3	61
144	Multi-modal Learning from Unpaired Images: Application to Multi-organ Segmentation in CT and MRI. , 2018, , .		61

#	Article	IF	CITATIONS
145	Cerebral atrophy measurements using Jacobian integration: Comparison with the boundary shift integral. NeuroImage, 2006, 32, 159-169.	4.2	60
146	Impaired development of the cerebral cortex in infants with congenital heart disease is correlated to reduced cerebral oxygen delivery. Scientific Reports, 2017, 7, 15088.	3.3	60
147	3-D Reconstruction in Canonical Co-Ordinate Space From Arbitrarily Oriented 2-D Images. IEEE Transactions on Medical Imaging, 2018, 37, 1737-1750.	8.9	60
148	Dynamic Changes in White Matter Abnormalities Correlate With Late Improvement and Deterioration Following TBI. Neurorehabilitation and Neural Repair, 2016, 30, 49-62.	2.9	59
149	Unsupervised Deformable Registration for Multi-modal Images via Disentangled Representations. Lecture Notes in Computer Science, 2019, , 249-261.	1.3	59
150	Data Efficient Unsupervised Domain Adaptation For Cross-modality Image Segmentation. Lecture Notes in Computer Science, 2019, , 669-677.	1.3	59
151	Classification and Lateralization of Temporal Lobe Epilepsies with and without Hippocampal Atrophy Based on Whole-Brain Automatic MRI Segmentation. PLoS ONE, 2012, 7, e33096.	2.5	59
152	Assessment of brain growth in early childhood using deformation-based morphometry. NeuroImage, 2008, 39, 348-358.	4.2	57
153	Al-Based Reconstruction for Fast MRI—A Systematic Review and Meta-Analysis. Proceedings of the IEEE, 2022, 110, 224-245.	21.3	57
154	Construction of a 4D Statistical Atlas of the Cardiac Anatomy and Its Use in Classification. Lecture Notes in Computer Science, 2005, 8, 402-410.	1.3	56
155	Stratified Decision Forests for Accurate Anatomical Landmark Localization in Cardiac Images. IEEE Transactions on Medical Imaging, 2017, 36, 332-342.	8.9	56
156	Phenotypic Expression and Outcomes in Individuals With Rare Genetic Variants of Hypertrophic Cardiomyopathy. Journal of the American College of Cardiology, 2021, 78, 1097-1110.	2.8	55
157	Hierarchical statistical shape analysis and prediction of sub-cortical brain structures. Medical Image Analysis, 2008, 12, 55-68.	11.6	54
158	Heterogeneity in Brain Microstructural Development Following Preterm Birth. Cerebral Cortex, 2020, 30, 4800-4810.	2.9	54
159	Simulation of cardiac pathologies using an electromechanical biventricular model and XMR interventional imaging. Medical Image Analysis, 2005, 9, 467-480.	11.6	53
160	Pathological Computed Tomography Features Associated With Adverse Outcomes After Mild Traumatic Brain Injury. JAMA Neurology, 2021, 78, 1137.	9.0	53
161	Classifier Selection Strategies for Label Fusion Using Large Atlas Databases. , 2007, 10, 523-531.		53
162	Medical imaging deep learning with differential privacy. Scientific Reports, 2021, 11, 13524.	3.3	52

#	Article	IF	CITATIONS
163	Automatic 3D ASM Construction via Atlas-Based Landmarking and Volumetric Elastic Registration. Lecture Notes in Computer Science, 2001, , 78-91.	1.3	51
164	Spatial Transformation of Motion and Deformation Fields Using Nonrigid Registration. IEEE Transactions on Medical Imaging, 2004, 23, 1065-1076.	8.9	50
165	Multi-organ Abdominal CT Segmentation Using Hierarchically Weighted Subject-Specific Atlases. Lecture Notes in Computer Science, 2012, 15, 10-17.	1.3	50
166	Nonlinear dimensionality reduction combining MR imaging with non-imaging information. Medical Image Analysis, 2012, 16, 819-830.	11.6	50
167	Temporal sparse free-form deformations. Medical Image Analysis, 2013, 17, 779-789.	11.6	50
168	Adversarial and Perceptual Refinement for Compressed Sensing MRI Reconstruction. Lecture Notes in Computer Science, 2018, , 232-240.	1.3	50
169	Nonrigid Registration of Medical Images: Theory, Methods, and Applications [Applications Corner. IEEE Signal Processing Magazine, 2010, 27, 113-119.	5.6	49
170	Structural MRI in Frontotemporal Dementia: Comparisons between Hippocampal Volumetry, Tensor-Based Morphometry and Voxel-Based Morphometry. PLoS ONE, 2012, 7, e52531.	2.5	49
171	Computational anatomy for multi-organ analysis in medical imaging: A review. Medical Image Analysis, 2019, 56, 44-67.	11.6	48
172	Water–fat Dixon cardiac magnetic resonance fingerprinting. Magnetic Resonance in Medicine, 2020, 83, 2107-2123.	3.0	48
173	Segmentation of Brain MRI in Young Children. Academic Radiology, 2007, 14, 1350-1366.	2.5	47
174	A dynamic approach to the recognition of 3D facial expressions and their temporal models. , 2011, , .		46
175	Reconstruction of a 3D surface from video that is robust to missing data and outliers: Application to minimally invasive surgery using stereo and mono endoscopes. Medical Image Analysis, 2012, 16, 597-611.	11.6	44
176	A Combined Manifold Learning Analysis of Shape and Appearance to Characterize Neonatal Brain Development. IEEE Transactions on Medical Imaging, 2011, 30, 2072-2086.	8.9	43
177	Common Genetic Variants and Risk of Brain Injury After Preterm Birth. Pediatrics, 2014, 133, e1655-e1663.	2.1	43
178	Brain Extraction Using Label Propagation and Group Agreement: Pincram. PLoS ONE, 2015, 10, e0129211.	2.5	43
179	Independent Left Ventricular Morphometric Atlases Show Consistent Relationships with Cardiovascular Risk Factors: A UK Biobank Study. Scientific Reports, 2019, 9, 1130.	3.3	43
180	Population-based studies of myocardial hypertrophy: high resolution cardiovascular magnetic resonance atlases improve statistical power. Journal of Cardiovascular Magnetic Resonance, 2014, 16, 16.	3.3	42

#	Article	IF	CITATIONS
181	Learning-Based Quality Control for Cardiac MR Images. IEEE Transactions on Medical Imaging, 2019, 38, 1127-1138.	8.9	42
182	Development of Microstructural and Morphological Cortical Profiles in the Neonatal Brain. Cerebral Cortex, 2020, 30, 5767-5779.	2.9	42
183	VS-Net: Variable Splitting Network for Accelerated Parallel MRI Reconstruction. Lecture Notes in Computer Science, 2019, , 713-722.	1.3	42
184	Multiple Sclerosis Lesion Segmentation Using Dictionary Learning and Sparse Coding. Lecture Notes in Computer Science, 2013, 16, 735-742.	1.3	42
185	The Developing Human Connectome Project Neonatal Data Release. Frontiers in Neuroscience, 2022, 16,	2.8	42
186	A prospective evaluation of cardiovascular magnetic resonance measures of dyssynchrony in the prediction of response to cardiac resynchronization therapy. Journal of Cardiovascular Magnetic Resonance, 2014, 16, 58.	3.3	41
187	Manifold population modeling as a neuro-imaging biomarker: Application to ADNI and ADNI-GO. NeuroImage, 2014, 94, 275-286.	4.2	41
188	Ventricular remodeling in preterm infants: computational cardiac magnetic resonance atlasing shows significant early remodeling of the left ventricle. Pediatric Research, 2019, 85, 807-815.	2.3	41
189	Precursors of Hypertensive Heart Phenotype Develop in Healthy Adults. JACC: Cardiovascular Imaging, 2015, 8, 1260-1269.	5.3	40
190	Preterm birth alters the development of cortical microstructure and morphology at term-equivalent age. NeuroImage, 2021, 243, 118488.	4.2	40
191	Comparison and Evaluation of Segmentation Techniques for Subcortical Structures in Brain MRI. Lecture Notes in Computer Science, 2008, 11, 409-416.	1.3	40
192	Video Summarization Through Reinforcement Learning With a 3D Spatio-Temporal U-Net. IEEE Transactions on Image Processing, 2022, 31, 1573-1586.	9.8	40
193	Differences between Men and Women in Treatment and Outcome after Traumatic Brain Injury. Journal of Neurotrauma, 2021, 38, 235-251.	3.4	39
194	Systematic evaluation of iterative deep neural networks for fast parallel MRI reconstruction with sensitivityâ€weighted coil combination. Magnetic Resonance in Medicine, 2021, 86, 1859-1872.	3.0	39
195	Group-wise parcellation of the cortex through multi-scale spectral clustering. NeuroImage, 2016, 136, 68-83.	4.2	38
196	Five-class differential diagnostics of neurodegenerative diseases using random undersampling boosting. Neurolmage: Clinical, 2017, 15, 613-624.	2.7	38
197	Brain lesion segmentation through image synthesis and outlier detection. Neurolmage: Clinical, 2017, 16, 643-658.	2.7	38
198	Automated Detection of Motion Artefacts in MR Imaging Using Decision Forests. Journal of Medical Engineering, 2017, 2017, 1-9.	1.1	38

#	Article	IF	CITATIONS
199	Weakly Supervised Estimation of Shadow Confidence Maps in Fetal Ultrasound Imaging. IEEE Transactions on Medical Imaging, 2019, 38, 2755-2767.	8.9	38
200	Cortical morphology at birth reflects spatiotemporal patterns of gene expression in the fetal human brain. PLoS Biology, 2020, 18, e3000976.	5.6	38
201	Human-level Performance On Automatic Head Biometrics In Fetal Ultrasound Using Fully Convolutional Neural Networks. , 2018, 2018, 714-717.		37
202	High-resolution dynamic MR imaging of the thorax for respiratory motion correction of PET using groupwise manifold alignment. Medical Image Analysis, 2014, 18, 939-952.	11.6	36
203	Cardiac Rhythm Device Identification Using Neural Networks. JACC: Clinical Electrophysiology, 2019, 5, 576-586.	3.2	36
204	Predicting the shapes of bones at a joint: application to the shoulder. Computer Methods in Biomechanics and Biomedical Engineering, 2008, 11, 19-30.	1.6	35
205	A framework for combining a motion atlas with non-motion information to learn clinically useful biomarkers: Application to cardiac resynchronisation therapy response prediction. Medical Image Analysis, 2017, 35, 669-684.	11.6	35
206	Learning Interpretable Anatomical Features Through Deep Generative Models: Application to Cardiac Remodeling. Lecture Notes in Computer Science, 2018, , 464-471.	1.3	35
207	Self-Supervised Learning for Few-Shot Medical Image Segmentation. IEEE Transactions on Medical Imaging, 2022, 41, 1837-1848.	8.9	35
208	Groupwise Combined Segmentation and Registration for Atlas Construction. , 2007, 10, 532-540.		34
209	Image guidance for robotic minimally invasive coronary artery bypass. Computerized Medical Imaging and Graphics, 2010, 34, 61-68.	5.8	34
210	Three-dimensional cardiovascular imaging-genetics: a mass univariate framework. Bioinformatics, 2018, 34, 97-103.	4.1	34
211	Explainable Anatomical Shape Analysis Through Deep Hierarchical Generative Models. IEEE Transactions on Medical Imaging, 2020, 39, 2088-2099.	8.9	34
212	Fast Multiple Landmark Localisation Using a Patch-Based Iterative Network. Lecture Notes in Computer Science, 2018, 2018, 563-571.	1.3	34
213	Multiple Landmark Detection Using Multi-agent Reinforcement Learning. Lecture Notes in Computer Science, 2019, , 262-270.	1.3	34
214	Fast Fully Automatic Segmentation of the Human Placenta from Motion Corrupted MRI. Lecture Notes in Computer Science, 2016, , 589-597.	1.3	34
215	Explaining Outcome Differences between Men and Women following Mild Traumatic Brain Injury. Journal of Neurotrauma, 2021, 38, 3315-3331.	3.4	34
216	Effect of frailty on 6-month outcome after traumatic brain injury: a multicentre cohort study with external validation. Lancet Neurology, The, 2022, 21, 153-162.	10.2	34

#	Article	IF	CITATIONS
217	Robustness of automated hippocampal volumetry across magnetic resonance field strengths and repeat images. Alzheimer's and Dementia, 2014, 10, 430.	0.8	33
218	PVR: Patch-to-Volume Reconstruction for Large Area Motion Correction of Fetal MRI. IEEE Transactions on Medical Imaging, 2017, 36, 2031-2044.	8.9	33
219	Graph Saliency Maps Through Spectral Convolutional Networks: Application toÂSex Classification with Brain Connectivity. Lecture Notes in Computer Science, 2018, , 3-13.	1.3	33
220	Optimizing the Diagnosis of Early Alzheimer's Disease in Mild Cognitive Impairment Subjects. Journal of Alzheimer's Disease, 2012, 32, 969-979.	2.6	32
221	Realistic Adversarial Data Augmentation for MR Image Segmentation. Lecture Notes in Computer Science, 2020, , 667-677.	1.3	32
222	Motion and deformation tracking for short-axis echo-planar myocardial perfusion imaging. Medical Image Analysis, 1998, 2, 285-302.	11.6	31
223	Fully automatic, multiorgan segmentation in normal whole body magnetic resonance imaging (<scp>MRI</scp>), using classification forests (<scp>CF</scp> s), convolutional neural networks (<scp>CNN</scp> s), and a multiâ€atlas (<scp>MA</scp>) approach. Medical Physics, 2017, 44, 5210-5220.	3.0	31
224	Improving ultrasound video classification: an evaluation of novel deep learning methods in echocardiography. Journal of Medical Artificial Intelligence, 2020, 3, 4-4.	1.1	31
225	Occurrence and timing of withdrawal of life-sustaining measures in traumatic brain injury patients: a CENTER-TBI study. Intensive Care Medicine, 2021, 47, 1115-1129.	8.2	31
226	Predicting Slice-to-Volume Transformation inÂPresence of Arbitrary Subject Motion. Lecture Notes in Computer Science, 2017, , 296-304.	1.3	31
227	Analysis of myocardial motion in tagged MR images using nonrigid image registration. , 2002, , .		30
228	Automated morphological analysis of magnetic resonance brain imaging using spectral analysis. Neurolmage, 2008, 43, 225-235.	4.2	30
229	Standard Plane Detection in 3D Fetal Ultrasound Using an Iterative Transformation Network. Lecture Notes in Computer Science, 2018, , 392-400.	1.3	30
230	Central versus Local Radiological Reading of Acute Computed Tomography Characteristics in Multi-Center Traumatic Brain Injury Research. Journal of Neurotrauma, 2019, 36, 1080-1092.	3.4	30
231	Model-Based and Data-Driven Strategies in Medical Image Computing. Proceedings of the IEEE, 2020, 108, 110-124.	21.3	30
232	Deep Learningâ€Based Automated Abdominal Organ Segmentation in the UK Biobank and German National Cohort Magnetic Resonance Imaging Studies. Investigative Radiology, 2021, 56, 401-408.	6.2	30
233	Manifold Learning for Medical Image Registration, Segmentation, and Classification. Advances in Bioinformatics and Biomedical Engineering Book Series, 2012, , 351-372.	0.4	30
234	Machine learning in knee arthroplasty: specific data are key—a systematic review. Knee Surgery, Sports Traumatology, Arthroscopy, 2022, 30, 376-388.	4.2	30

#	Article	IF	CITATIONS
235	Precision measurement of cardiac structure and function in cardiovascular magnetic resonance using machine learning. Journal of Cardiovascular Magnetic Resonance, 2022, 24, 16.	3.3	30
236	Nonrigid Registration. Biomedical Engineering Series, 2001, , 281-301.	0.4	29
237	A Framework for Inter-Subject Prediction of Functional Connectivity From Structural Networks. IEEE Transactions on Medical Imaging, 2013, 32, 2200-2214.	8.9	29
238	A deformable model for the reconstruction of the neonatal cortex. , 2017, , .		29
239	Data-Driven Differential Diagnosis of Dementia Using Multiclass Disease State Index Classifier. Frontiers in Aging Neuroscience, 2018, 10, 111.	3.4	29
240	Geodesic Patch-Based Segmentation. Lecture Notes in Computer Science, 2014, 17, 666-673.	1.3	29
241	Serum metabolome associated with severity of acute traumatic brain injury. Nature Communications, 2022, 13, 2545.	12.8	29
242	Fast calculation of digitally reconstructed radiographs using light fields. , 2003, , .		28
243	Mutual Information-Based Disentangled Neural Networks for Classifying Unseen Categories in Different Domains: Application to Fetal Ultrasound Imaging. IEEE Transactions on Medical Imaging, 2021, 40, 722-734.	8.9	28
244	Learning Shape Priors for Robust Cardiac MR Segmentation from Multi-view Images. Lecture Notes in Computer Science, 2019, , 523-531.	1.3	28
245	Geodesic Information Flows. Lecture Notes in Computer Science, 2012, 15, 262-270.	1.3	27
246	Joint Spectral Decomposition for the Parcellation of the Human Cerebral Cortex Using Resting-State fMRI. Lecture Notes in Computer Science, 2015, 24, 85-97.	1.3	27
247	<scp>T1</scp> , <scp>T2,</scp> and Fat Fraction Cardiac MR Fingerprinting: Preliminary Clinical Evaluation. Journal of Magnetic Resonance Imaging, 2021, 53, 1253-1265.	3.4	27
248	Automatic View Planning with Multi-scale Deep Reinforcement Learning Agents. Lecture Notes in Computer Science, 2018, , 277-285.	1.3	27
249	Testing the Sensitivity of Tract-Based Spatial Statistics to Simulated Treatment Effects in Preterm Neonates. PLoS ONE, 2013, 8, e67706.	2.5	27
250	Three-dimensional cardiovascular image analysis. IEEE Transactions on Medical Imaging, 2002, 21, 1005-1010.	8.9	26
251	Generalised Overlap Measures for Assessment of Pairwise and Groupwise Image Registration and Segmentation. Lecture Notes in Computer Science, 2005, 8, 99-106.	1.3	26
252	Analysis of serial magnetic resonance images of mouse brains using image registration. Neurolmage, 2009, 44, 692-700.	4.2	26

#	Article	IF	CITATIONS
253	The PredictAD project: development of novel biomarkers and analysis software for early diagnosis of the Alzheimer's disease. Interface Focus, 2013, 3, 20120072.	3.0	26
254	Hierarchical Manifold Learning for Regional Image Analysis. IEEE Transactions on Medical Imaging, 2014, 33, 444-461.	8.9	26
255	Adversarial interference and its mitigations in privacy-preserving collaborative machine learning. Nature Machine Intelligence, 2021, 3, 749-758.	16.0	26
256	Similarity Metrics for Groupwise Non-rigid Registration. , 2007, 10, 544-552.		26
257	Surgery versus conservative treatment for traumatic acute subdural haematoma: a prospective, multicentre, observational, comparative effectiveness study. Lancet Neurology, The, 2022, 21, 620-631.	10.2	26
258	A multivariate statistical analysis of the developing human brain in preterm infants. Image and Vision Computing, 2007, 25, 981-994.	4.5	25
259	Super-resolution reconstruction of cardiac MRI using coupled dictionary learning. , 2014, , .		25
260	Autoadaptive motion modelling for MR-based respiratory motion estimation. Medical Image Analysis, 2017, 35, 83-100.	11.6	25
261	Regional brain morphometry in patients with traumatic brain injury based on acute- and chronic-phase magnetic resonance imaging. PLoS ONE, 2017, 12, e0188152.	2.5	25
262	Fibrosis Microstructure Modulates Reentry in Non-ischemic Dilated Cardiomyopathy: Insights From Imaged Guided 2D Computational Modeling. Frontiers in Physiology, 2018, 9, 1832.	2.8	25
263	Rapid Automated Quantification of Cerebral Leukoaraiosis on CT Images: A Multicenter Validation Study. Radiology, 2018, 288, 573-581.	7.3	25
264	A Framework for Detailed Objective Comparison of Non-rigid Registration Algorithms in Neuroimaging. Lecture Notes in Computer Science, 2004, , 679-686.	1.3	25
265	Remodeling after acute myocardial infarction: mapping ventricular dilatation using three dimensional CMR image registration. Journal of Cardiovascular Magnetic Resonance, 2012, 14, 46.	3.3	24
266	4D Blood Flow Reconstruction Over the Entire Ventricle From Wall Motion and Blood Velocity Derived From Ultrasound Data. IEEE Transactions on Medical Imaging, 2015, 34, 2298-2308.	8.9	24
267	Brain Connectivity Measures Improve Modeling of Functional Outcome After Acute Ischemic Stroke. Stroke, 2019, 50, 2761-2767.	2.0	24
268	Relationship between body composition and left ventricular geometry using three dimensional cardiovascular magnetic resonance. Journal of Cardiovascular Magnetic Resonance, 2016, 18, 32.	3.3	23
269	Real-Time Prediction of Segmentation Quality. Lecture Notes in Computer Science, 2018, , 578-585.	1.3	23
270	Impact of a clinical decision support tool on prediction of progression in early-stage dementia: a prospective validation study. Alzheimer's Research and Therapy, 2019, 11, 25.	6.2	23

#	Article	IF	CITATIONS
271	Impact of a Clinical Decision Support Tool on Dementia Diagnostics in Memory Clinics: The PredictND Validation Study. Current Alzheimer Research, 2019, 16, 91-101.	1.4	23
272	Modelling the progression of Alzheimer's disease in MRI using generative adversarial networks. , 2018, , .		23
273	Medical Image Registration. Biological and Medical Physics Series, 2010, , 131-154.	0.4	22
274	Development of the Corticospinal and Callosal Tracts from Extremely Premature Birth up to 2 Years of Age. PLoS ONE, 2015, 10, e0125681.	2.5	22
275	Learning clinically useful information from images: Past, present and future. Medical Image Analysis, 2016, 33, 13-18.	11.6	22
276	Bayesian Deep Learning for Accelerated MR Image Reconstruction. Lecture Notes in Computer Science, 2018, , 64-71.	1.3	22
277	Impact of Antithrombotic Agents on Radiological Lesion Progression in Acute Traumatic Brain Injury: A CENTER-TBI Propensity-Matched Cohort Analysis. Journal of Neurotrauma, 2020, 37, 2069-2080.	3.4	22
278	Large-scale Quality Control of Cardiac Imaging in Population Studies: Application to UK Biobank. Scientific Reports, 2020, 10, 2408.	3.3	22
279	Stochastic Deep Compressive Sensing for the Reconstruction of Diffusion Tensor Cardiac MRI. Lecture Notes in Computer Science, 2018, , 295-303.	1.3	22
280	Cardiac segmentation on late gadolinium enhancement MRI: A benchmark study from multi-sequence cardiac MR segmentation challenge. Medical Image Analysis, 2022, 81, 102528.	11.6	22
281	Multivariate Statistical Differences of MRI Samples of the Human Brain. Journal of Mathematical Imaging and Vision, 2007, 29, 95-106.	1.3	21
282	Supervoxel classification forests for estimating pairwise image correspondences. Pattern Recognition, 2017, 63, 561-569.	8.1	21
283	Global Characterisation of Coagulopathy in Isolated Traumatic Brain Injury (iTBI): A CENTER-TBI Analysis. Neurocritical Care, 2021, 35, 184-196.	2.4	21
284	Complementary timeâ€frequency domain networks for dynamic parallel MR image reconstruction. Magnetic Resonance in Medicine, 2021, 86, 3274-3291.	3.0	21
285	Learning Biomarker Models for Progression Estimation of Alzheimer's Disease. PLoS ONE, 2016, 11, e0153040.	2.5	21
286	Multi-class brain segmentation using atlas propagation and EM-based refinement. , 2012, , .		20
287	Distortion Correction in Fetal EPI Using Non-Rigid Registration With a Laplacian Constraint. IEEE Transactions on Medical Imaging, 2018, 37, 12-19.	8.9	20
288	Deep learning with ultrasound physics for fetal skull segmentation. , 2018, , .		20

#	Article	IF	CITATIONS
289	Prediction of Global Functional Outcome and Post-Concussive Symptoms after Mild Traumatic Brain Injury: External Validation of Prognostic Models in the Collaborative European NeuroTrauma Effectiveness Research in Traumatic Brain Injury (CENTER-TBI) Study. Journal of Neurotrauma, 2021, 38, 196-209.	3.4	20
290	Regression Forest-Based Atlas Localization and Direction Specific Atlas Generation for Pancreas Segmentation. Lecture Notes in Computer Science, 2016, , 556-563.	1.3	20
291	Simultaneous Fine and Coarse Diffeomorphic Registration: Application to Atrophy Measurement in Alzheimer's Disease. Lecture Notes in Computer Science, 2010, 13, 610-617.	1.3	20
292	A Probabilistic Framework to Infer Brain Functional Connectivity from Anatomical Connections. Lecture Notes in Computer Science, 2011, 22, 296-307.	1.3	20
293	Prediction of complications and surgery duration in primary TKA with high accuracy using machine learning with arthroplasty-specific data. Knee Surgery, Sports Traumatology, Arthroscopy, 2023, 31, 1323-1333.	4.2	20
294	Localisation of the Brain in Fetal MRI Using Bundled SIFT Features. Lecture Notes in Computer Science, 2013, 16, 582-589.	1.3	19
295	Pseudo-healthy Image Synthesis for White Matter Lesion Segmentation. Lecture Notes in Computer Science, 2016, , 87-96.	1.3	19
296	Automatic MRI Quantifying Methods in Behavioral-Variant Frontotemporal Dementia Diagnosis. Dementia and Geriatric Cognitive Disorders Extra, 2018, 8, 51-59.	1.3	19
297	A large margin algorithm for automated segmentation of white matter hyperintensity. Pattern Recognition, 2018, 77, 150-159.	8.1	19
298	Evaluating combinations of diagnostic tests to discriminate different dementia types. Alzheimer's and Dementia: Diagnosis, Assessment and Disease Monitoring, 2018, 10, 509-518.	2.4	19
299	Tracheal intubation in traumatic brain injury: a multicentre prospective observational study. British Journal of Anaesthesia, 2020, 125, 505-517.	3.4	19
300	Phenotyping the Preterm Brain: Characterizing Individual Deviations From Normative Volumetric Development in Two Large Infant Cohorts. Cerebral Cortex, 2021, 31, 3665-3677.	2.9	19
301	Tractography-Driven Groupwise Multi-scale Parcellation of the Cortex. Lecture Notes in Computer Science, 2015, 24, 600-612.	1.3	19
302	T2* relaxometry of fetal brain at 1.5 Tesla using a motion tolerant method. Magnetic Resonance in Medicine, 2015, 73, 1795-1802.	3.0	18
303	3D Fetal Skull Reconstruction from 2DUS via Deep Conditional Generative Networks. Lecture Notes in Computer Science, 2018, , 383-391.	1.3	18
304	Cardiac MR Motion Artefact Correction from K-space Using Deep Learning-Based Reconstruction. Lecture Notes in Computer Science, 2018, , 21-29.	1.3	18
305	A dataâ€driven approach to optimising the encoding for multiâ€shell diffusion MRI with application to neonatal imaging. NMR in Biomedicine, 2020, 33, e4348.	2.8	18
306	De Novo Radiomics Approach Using Image Augmentation and Features From T1 Mapping to Predict Gleason Scores in Prostate Cancer. Investigative Radiology, 2021, 56, 661-668.	6.2	18

#	Article	IF	CITATIONS
307	k-t NEXT: Dynamic MR Image Reconstruction Exploiting Spatio-Temporal Correlations. Lecture Notes in Computer Science, 2019, , 505-513.	1.3	18
308	Motion Corrected 3D Reconstruction of the Fetal Thorax from Prenatal MRI. Lecture Notes in Computer Science, 2014, 17, 284-291.	1.3	18
309	Manifold Alignment and Transfer Learning for Classification of Alzheimer's Disease. Lecture Notes in Computer Science, 2014, , 77-84.	1.3	18
310	sPLINK: a hybrid federated tool as a robust alternative to meta-analysis in genome-wide association studies. Genome Biology, 2022, 23, 32.	8.8	18
311	Using a Maximum Uncertainty LDA-Based Approach to Classify and Analyse MR Brain Images. Lecture Notes in Computer Science, 2004, , 291-300.	1.3	17
312	Automatic volumetry on MR brain images can support diagnostic decision making. BMC Medical Imaging, 2008, 8, 9.	2.7	17
313	Construction of a patient-specific atlas of the brain: Application to normal aging. , 2008, , .		17
314	Understanding the need of ventricular pressure for the estimation of diastolic biomarkers. Biomechanics and Modeling in Mechanobiology, 2014, 13, 747-757.	2.8	17
315	Evaluating Imputation Techniques for Missing Data in ADNI: A Patient Classification Study. Lecture Notes in Computer Science, 2015, , 3-10.	1.3	17
316	Investigating altered brain development in infants with congenital heart disease using tensor-based morphometry. Scientific Reports, 2020, 10, 14909.	3.3	17
317	Deep Nested Level Sets: Fully Automated Segmentation of Cardiac MR Images in Patients with Pulmonary Hypertension. Lecture Notes in Computer Science, 2018, , 595-603.	1.3	17
318	Ultrasound Video Summarization Using Deep Reinforcement Learning. Lecture Notes in Computer Science, 2020, , 483-492.	1.3	17
319	Evaluation of Rigid and Non-rigid Motion Compensation of Cardiac Perfusion MRI. Lecture Notes in Computer Science, 2008, 11, 35-43.	1.3	17
320	A Computational White Matter Atlas for Aging with Surface-Based Representation of Fasciculi. Lecture Notes in Computer Science, 2010, , 83-90.	1.3	17
321	Automatic Segmentation of Different Pathologies from Cardiac Cine MRI Using Registration and Multiple Component EM Estimation. Lecture Notes in Computer Science, 2011, , 163-170.	1.3	17
322	Manifold Learning for Biomarker Discovery in MR Imaging. Lecture Notes in Computer Science, 2010, , 116-123.	1.3	16
323	Automatical vessel wall detection in intravascular coronary OCT. , 2011, , .		16

Regional analysis of FDG-PET for use in the classification of Alzheimer'S Disease. , 2011, , .

#	Article	IF	CITATIONS
325	Small Organ Segmentation in Whole-Body MRI Using a Two-Stage FCN and Weighting Schemes. Lecture Notes in Computer Science, 2018, , 346-354.	1.3	16
326	Missing Data in Prediction Research: A Five-Step Approach for Multiple Imputation, Illustrated in the CENTER-TBI Study. Journal of Neurotrauma, 2021, 38, 1842-1857.	3.4	16
327	Incidental findings on brain MR imaging of asymptomatic term neonates in the Developing Human Connectome Project. EClinicalMedicine, 2021, 38, 100984.	7.1	16
328	Al for Doctors—A Course to Educate Medical Professionals in Artificial Intelligence for Medical Imaging. Healthcare (Switzerland), 2021, 9, 1278.	2.0	16
329	Detection and Correction of Cardiac MRI Motion Artefacts During Reconstruction from k-space. Lecture Notes in Computer Science, 2019, , 695-703.	1.3	16
330	Fully Automated Segmentation-Based Respiratory Motion Correction of Multiplanar Cardiac Magnetic Resonance Images for Large-Scale Datasets. Lecture Notes in Computer Science, 2017, , 332-340.	1.3	16
331	Automatic Cortical Segmentation in the Developing Brain. Lecture Notes in Computer Science, 2007, 20, 257-269.	1.3	16
332	Random Forest-Based Manifold Learning for Classification of Imaging Data in Dementia. Lecture Notes in Computer Science, 2011, , 159-166.	1.3	16
333	Exploring a new paradigm for the fetal anomaly ultrasound scan: Artificial intelligence in real time. Prenatal Diagnosis, 2022, 42, 49-59.	2.3	16
334	Automatic Quantification of Changes in Bone in Serial MR Images of Joints. IEEE Transactions on Medical Imaging, 2006, 25, 1617-1626.	8.9	15
335	Cardiac MR Segmentation from Undersampled k-space Using Deep Latent Representation Learning. Lecture Notes in Computer Science, 2018, , 259-267.	1.3	15
336	Exploiting Motion for Deep Learning Reconstruction of Extremely-Undersampled Dynamic MRI. Lecture Notes in Computer Science, 2019, , 704-712.	1.3	15
337	Nonrigid Image Registration with Subdivision Lattices: Application to Cardiac MR Image Analysis. , 2007, 10, 335-342.		15
338	Non-rigid Reconstruction of the Beating Heart Surface for Minimally Invasive Cardiac Surgery. Lecture Notes in Computer Science, 2009, 12, 34-42.	1.3	15
339	Dense Multi-frame Optic Flow for Non-rigid Objects Using Subspace Constraints. Lecture Notes in Computer Science, 2011, , 460-473.	1.3	15
340	Beyond theg-factor limit in sensitivity encoding using joint histogram entropy. Magnetic Resonance in Medicine, 2006, 55, 153-160.	3.0	14
341	Automated measurement of local white matter lesion volume. NeuroImage, 2012, 59, 3901-3908.	4.2	14
342	Software Tool for Improved Prediction of Alzheimer's Disease. Neurodegenerative Diseases, 2012, 10, 149-152.	1.4	14

#	Article	IF	CITATIONS
343	Nonlinear Graph Fusion for Multi-modal Classification of Alzheimer's Disease. Lecture Notes in Computer Science, 2015, , 77-84.	1.3	14
344	Joint Motion Estimation and Segmentation from Undersampled Cardiac MR Image. Lecture Notes in Computer Science, 2018, , 55-63.	1.3	14
345	Reduced structural connectivity in cortico-striatal-thalamic network in neonates with congenital heart disease. NeuroImage: Clinical, 2020, 28, 102423.	2.7	14
346	Statistical Finite Element Model for Bone Shape and Biomechanical Properties. Lecture Notes in Computer Science, 2006, 9, 405-411.	1.3	14
347	An Automatic Data Assimilation Framework for Patient-Specific Myocardial Mechanical Parameter Estimation. Lecture Notes in Computer Science, 2011, , 392-400.	1.3	14
348	Interpretable Deep Models for Cardiac Resynchronisation Therapy Response Prediction. Lecture Notes in Computer Science, 2020, 2020, 284-293.	1.3	14
349	Multi-atlas Segmentation as a Graph Labelling Problem: Application to Partially Annotated Atlas Data. Lecture Notes in Computer Science, 2015, 24, 221-232.	1.3	13
350	Multi-stage Biomarker Models for Progression Estimation in Alzheimer's Disease. Lecture Notes in Computer Science, 2015, 24, 387-398.	1.3	13
351	Deep Learning Using K-Space Based Data Augmentation for Automated Cardiac MR Motion Artefact Detection. Lecture Notes in Computer Science, 2018, , 250-258.	1.3	13
352	LSTM Spatial Co-transformer Networks for Registration of 3D Fetal US and MR Brain Images. Lecture Notes in Computer Science, 2018, , 149-159.	1.3	13
353	Metabolic pathways associated with right ventricular adaptation to pulmonary hypertension: 3D analysis of cardiac magnetic resonance imaging. European Heart Journal Cardiovascular Imaging, 2019, 20, 668-676.	1.2	13
354	Late-Gadolinium Enhancement Interface Area and Electrophysiological Simulations Predict Arrhythmic Events in Patients With Nonischemic Dilated Cardiomyopathy. JACC: Clinical Electrophysiology, 2021, 7, 238-249.	3.2	13
355	Spatio-temporal Alignment of 4D Cardiac MR Images. Lecture Notes in Computer Science, 2003, , 205-214.	1.3	13
356	Groupwise Simultaneous Manifold Alignment for High-Resolution Dynamic MR Imaging of Respiratory Motion. Lecture Notes in Computer Science, 2013, 23, 232-243.	1.3	13
357	Multi-channel MRI segmentation of eye structures and tumors using patient-specific features. PLoS ONE, 2017, 12, e0173900.	2.5	13
358	The relationship between lateral meniscus shape and joint contact parameters in the knee: a study using data from the Osteoarthritis Initiative. Arthritis Research and Therapy, 2014, 16, R27.	3.5	12
359	Patch-Based Evaluation of Image Segmentation. , 2014, , .		12
360	Identification of Cerebral Small Vessel Disease Using Multiple Instance Learning. Lecture Notes in Computer Science, 2015, , 523-530.	1.3	12

#	Article	IF	CITATIONS
361	Automatic Quality Control of Cardiac MRI Segmentation in Large-Scale Population Imaging. Lecture Notes in Computer Science, 2017, , 720-727.	1.3	12
362	Limited One-time Sampling Irregularity Map (LOTS-IM) for Automatic Unsupervised Assessment of White Matter Hyperintensities and Multiple Sclerosis Lesions in Structural Brain Magnetic Resonance Images. Computerized Medical Imaging and Graphics, 2020, 79, 101685.	5.8	12
363	Predictors of Access to Rehabilitation in the Year Following Traumatic Brain Injury: A European Prospective and Multicenter Study. Neurorehabilitation and Neural Repair, 2020, 34, 814-830.	2.9	12
364	Parental age effects on neonatal white matter development. NeuroImage: Clinical, 2020, 27, 102283.	2.7	12
365	Frequency of fatigue and its changes in the first 6Âmonths after traumatic brain injury: results from the CENTER-TBI study. Journal of Neurology, 2021, 268, 61-73.	3.6	12
366	Cooperative Training and Latent Space Data Augmentation for Robust Medical Image Segmentation. Lecture Notes in Computer Science, 2021, , 149-159.	1.3	12
367	Computing CNN Loss and Gradients for Pose Estimation with Riemannian Geometry. Lecture Notes in Computer Science, 2018, , 756-764.	1.3	12
368	Intelligent Image Synthesis to Attack a Segmentation CNN Using Adversarial Learning. Lecture Notes in Computer Science, 2019, , 90-99.	1.3	12
369	Patch-Based Segmentation without Registration: Application to Knee MRI. Lecture Notes in Computer Science, 2013, , 98-105.	1.3	12
370	Application-Driven MRI: Joint Reconstruction and Segmentation from Undersampled MRI Data. Lecture Notes in Computer Science, 2014, 17, 106-113.	1.3	12
371	Multivariate Statistical Analysis of Whole Brain Structural Networks Obtained Using Probabilistic Tractography. Lecture Notes in Computer Science, 2008, 11, 486-493.	1.3	12
372	A Systematic Comparison of Encrypted Machine Learning Solutions for Image Classification. , 2020, , .		12
373	Genetic and environmental determinants of diastolic heart function. , 2022, 1, 361-371.		12
374	Segmentation of cardiac MR and CT image sequences using model-based registration of a 4D statistical model. , 2007, , .		11
375	LISA: Longitudinal image registration via spatio-temporal atlases. , 2012, , .		11
376	Modeling of the bony pelvis from MRI using a multi-atlas AE-SDM for registration and tracking in image-guided robotic prostatectomy. Computerized Medical Imaging and Graphics, 2013, 37, 183-194.	5.8	11
377	Self-Aligning Manifolds for Matching Disparate Medical Image Datasets. Lecture Notes in Computer Science, 2015, 24, 363-374.	1.3	11
378	3D High-Resolution Cardiac Segmentation Reconstruction From 2D Views Using Conditional Variational Autoencoders. , 2019, , .		11

#	Article	IF	CITATIONS
379	Patch-Based Brain Age Estimation fromÂMRÂlmages. Lecture Notes in Computer Science, 2020, , 98-107.	1.3	11
380	Hierarchical Manifold Learning. Lecture Notes in Computer Science, 2012, 15, 512-519.	1.3	11
381	Neonatal multi-modal cortical profiles predict 18-month developmental outcomes. Developmental Cognitive Neuroscience, 2022, 54, 101103.	4.0	11
382	Predicting age and clinical risk from the neonatal connectome. NeuroImage, 2022, 257, 119319.	4.2	11
383	Health care utilization and outcomes in older adults after Traumatic Brain Injury: A CENTER-TBI study. Injury, 2022, 53, 2774-2782.	1.7	11
384	3D/4D Cardiac Segmentation Using Active Appearance Models, Non-rigid Registration, and the Insight Toolkit. Lecture Notes in Computer Science, 2004, , 419-426.	1.3	10
385	XMR guided cardiac electrophysiology study and radio frequency ablation. , 2004, 5369, 10.		10
386	Inference of functional connectivity from direct and indirect structural brain connections. , 2011, , .		10
387	Scar shape analysis and simulated electrical instabilities in a non-ischemic dilated cardiomyopathy patient cohort. PLoS Computational Biology, 2019, 15, e1007421.	3.2	10
388	Prognostic Validation of the NINDS Common Data Elements for the Radiologic Reporting of Acute Traumatic Brain Injuries: A CENTER-TBI Study. Journal of Neurotrauma, 2020, 37, 1269-1282.	3.4	10
389	Discriminating electrocardiographic responses to His-bundle pacing using machine learning. Cardiovascular Digital Health Journal, 2020, 1, 11-20.	1.3	10
390	Spatio-Temporal Free-Form Registration of Cardiac MR Image Sequences. Lecture Notes in Computer Science, 2004, , 911-919.	1.3	10
391	In-utero Three Dimension High Resolution Fetal Brain Diffusion Tensor Imaging. , 2007, 10, 18-26.		10
392	Flimma: a federated and privacy-aware tool for differential gene expression analysis. Genome Biology, 2021, 22, 338.	8.8	10
393	Multi-organ segmentation from 3D abdominal CT images using patient-specific weighted-probabilistic atlas. Proceedings of SPIE, 2013, , .	0.8	9
394	Learning and combining image neighborhoods using random forests for neonatal brain disease classification. Medical Image Analysis, 2017, 42, 189-199.	11.6	9
395	Learning a Model-Driven Variational Network for Deformable Image Registration. IEEE Transactions on Medical Imaging, 2022, 41, 199-212.	8.9	9
396	Joint Motion Correction and Super Resolution for Cardiac Segmentation viaÂLatent Optimisation. Lecture Notes in Computer Science, 2021, , 14-24.	1.3	9

#	Article	IF	CITATIONS
397	Efficient, high-performance semantic segmentation using multi-scale feature extraction. PLoS ONE, 2021, 16, e0255397.	2.5	9
398	Biomechanics-Informed Neural Networks for Myocardial Motion Tracking in MRI. Lecture Notes in Computer Science, 2020, , 296-306.	1.3	9
399	Deep Generative Model-Based Quality Control for Cardiac MRI Segmentation. Lecture Notes in Computer Science, 2020, , 88-97.	1.3	9
400	Image-Level Harmonization of Multi-site Data Using Image-and-Spatial Transformer Networks. Lecture Notes in Computer Science, 2020, , 710-719.	1.3	9
401	Multi-Level Parcellation of the Cerebral Cortex Using Resting-State fMRI. Lecture Notes in Computer Science, 2015, , 47-54.	1.3	9
402	Spatially Aware Patch-Based Segmentation (SAPS): An Alternative Patch-Based Segmentation Framework. Lecture Notes in Computer Science, 2013, , 93-103.	1.3	9
403	Multiple Instance Learning for Classification of Dementia in Brain MRI. Lecture Notes in Computer Science, 2013, 16, 599-606.	1.3	9
404	Developing and validating a multivariable prediction model which predicts progression of intermediate to late age-related macular degeneration—the PINNACLE trial protocol. Eye, 2023, 37, 1275-1283.	2.1	9
405	Tracking developmental changes in subcortical structures of the preterm brain using multi-modal MRI. , 2011, , .		8
406	A new automated system to identify a consistent sampling position to make tissue Doppler and transmitral Doppler measurements of E, E′ and E/E′. International Journal of Cardiology, 2012, 155, 394-399.	1.7	8
407	Multi-Atlas Segmentation Using Partially Annotated Data: Methods and Annotation Strategies. IEEE Transactions on Pattern Analysis and Machine Intelligence, 2018, 40, 1683-1696.	13.9	8
408	Evaluating severity of white matter lesions from computed tomography images with convolutional neural network. Neuroradiology, 2020, 62, 1257-1263.	2.2	8
409	Primary versus early secondary referral to a specialized neurotrauma center in patients with moderate/severe traumatic brain injury: a CENTER TBI study. Scandinavian Journal of Trauma, Resuscitation and Emergency Medicine, 2021, 29, 113.	2.6	8
410	Detecting Hypo-plastic Left Heart Syndrome in Fetal Ultrasound via Disease-Specific Atlas Maps. Lecture Notes in Computer Science, 2021, , 207-217.	1.3	8
411	Communicative Reinforcement Learning Agents for Landmark Detection in Brain Images. Lecture Notes in Computer Science, 2020, , 177-186.	1.3	8
412	Prospective Identification of CRT Super Responders Using a Motion Atlas and Random Projection Ensemble Learning. Lecture Notes in Computer Science, 2015, , 493-500.	1.3	8
413	A Robust Mosaicing Method with Super-Resolution for Optical Medical Images. Lecture Notes in Computer Science, 2010, , 373-382.	1.3	8
414	Informed consent procedures in patients with an acute inability to provide informed consent: Policy and practice in the CENTER-TBI study. Journal of Critical Care, 2020, 59, 6-15.	2.2	8

#	Article	IF	CITATIONS
415	Motion-Guided Physics-Based Learning for Cardiac MRI Reconstruction. , 2021, , .		8
416	Segmentation of subcortical structures and the hippocampus in brain MRI using graph-cuts and subject-specific a-priori information. , 2009, , .		7
417	Inference of functional connectivity from structural brain connectivity. , 2010, , .		7
418	Registration and Segmentation in Medical Imaging. Studies in Computational Intelligence, 2014, , 137-156.	0.9	7
419	Coronary centerline extraction based on ostium detection and model-guided directional minimal path. , 2014, , .		7
420	A robust similarity measure for volumetric image registration withÂoutliers. Image and Vision Computing, 2016, 52, 97-113.	4.5	7
421	A flexible graphical model for multi-modal parcellation of the cortex. NeuroImage, 2017, 162, 226-248.	4.2	7
422	Myocardial strain computed at multiple spatial scales from tagged magnetic resonance imaging: Estimating cardiac biomarkers for CRT patients. Medical Image Analysis, 2018, 43, 169-185.	11.6	7
423	Sex and regional differences in myocardial plasticity in aortic stenosis are revealed by 3D model machine learning. European Heart Journal Cardiovascular Imaging, 2019, 21, 417-427.	1.2	7
424	Dynamic Spatio-Temporal Graph Convolutional Networks For Cardiac Motion Analysis. , 2021, , .		7
425	Multi-atlas Spectral PatchMatch: Application to Cardiac Image Segmentation. Lecture Notes in Computer Science, 2014, 17, 348-355.	1.3	7
426	Flexible Reconstruction and Correction of Unpredictable Motion from Stacks ofÂ2D Images. Lecture Notes in Computer Science, 2015, , 555-562.	1.3	7
427	Automatic Segmentation of Left Atrial Scar from Delayed-Enhancement Magnetic Resonance Imaging. Lecture Notes in Computer Science, 2011, , 63-70.	1.3	7
428	Model-Guided Directional Minimal Path for Fully Automatic Extraction of Coronary Centerlines from Cardiac CTA. Lecture Notes in Computer Science, 2013, 16, 542-549.	1.3	7
429	Eidolon: Visualization and Computational Framework for Multi-modal Biomedical Data Analysis. Lecture Notes in Computer Science, 2016, , 425-437.	1.3	7
430	Prediction of Complications and Surgery Duration in Primary Total Hip Arthroplasty Using Machine Learning: The Necessity of Modified Algorithms and Specific Data. Journal of Clinical Medicine, 2022, 11, 2147.	2.4	7
431	<title>Multiscale approach to contour fitting for MR images</title> . , 1996, , .		6
432	Augmented reality image guidance for minimally invasive coronary artery bypass. Proceedings of SPIE, 2008, , .	0.8	6

#	Article	IF	CITATIONS
433	Towards dense motion estimation in light and electron microscopy. , 2011, , .		6
434	Manifold learning combining imaging with non-imaging information. , 2011, , .		6
435	Graph-Based Label Propagation in Fetal Brain MR Images. Lecture Notes in Computer Science, 2014, , 9-16.	1.3	6
436	Supervoxel Classification Forests for Estimating Pairwise Image Correspondences. Lecture Notes in Computer Science, 2015, , 94-101.	1.3	6
437	Regional Differences in End-Diastolic Volumes between 3D Echo and CMR in HLHS Patients. Frontiers in Pediatrics, 2016, 4, 133.	1.9	6
438	Automatic Shadow Detection in 2D Ultrasound Images. Lecture Notes in Computer Science, 2018, , 66-75.	1.3	6
439	Automated analysis and detection of abnormalities in transaxial anatomical cardiovascular magnetic resonance images: a proof of concept study with potential to optimize image acquisition. International Journal of Cardiovascular Imaging, 2021, 37, 1033-1042.	1.5	6
440	Deep Learning for Cardiac Motion Estimation: Supervised vs. Unsupervised Training. Lecture Notes in Computer Science, 2020, , 186-194.	1.3	6
441	Fast Reconstruction of Accelerated Dynamic MRI Using Manifold Kernel Regression. Lecture Notes in Computer Science, 2015, , 510-518.	1.3	6
442	GraMPa: Graph-Based Multi-modal Parcellation of the Cortex Using Fusion Moves. Lecture Notes in Computer Science, 2016, , 148-156.	1.3	6
443	Simulation of the Electromechanical Activity of the Heart Using XMR Interventional Imaging. Lecture Notes in Computer Science, 2004, , 786-794.	1.3	6
444	Non-rigid Spatio-Temporal Alignment of 4D Cardiac MR Images. Lecture Notes in Computer Science, 2003, , 191-200.	1.3	6
445	Laplacian Eigenmaps Manifold Learning for Landmark Localization in Brain MR Images. Lecture Notes in Computer Science, 2011, 14, 566-573.	1.3	6
446	Unsupervised Learning of Shape Complexity: Application to Brain Development. Lecture Notes in Computer Science, 2012, , 88-99.	1.3	6
447	A Novel Algorithm for Heart Motion Analysis Based on Geometric Constraints. Lecture Notes in Computer Science, 2008, 11, 720-728.	1.3	6
448	Solving MRF Minimization by Mirror Descent. Lecture Notes in Computer Science, 2012, , 587-598.	1.3	6
449	Harnessing feature extraction capacities from a pre-trained convolutional neural network (VGG-16) for the unsupervised distinction of aortic outflow velocity profiles in patients with severe aortic stenosis. European Heart Journal Digital Health, 2022, 3, 153-168.	1.7	6

450 Detecting regional changes in myocardial contraction patterns using MRI. , 2004, , .

4

#	Article	IF	CITATIONS
451	Atlas selection strategy for automatic segmentation of pediatric brain MRIs into 83 ROIs. , 2010, , .		5
452	Construction of a neonatal cortical surface atlas using multimodal surface matching. , 2016, , .		5
453	An exploration of task based fMRI in neonates using echo-shifting to allow acquisition at longer T E without loss of temporal efficiency. NeuroImage, 2016, 127, 298-306.	4.2	5
454	Exploring heritability of functional brain networks with inexact graph matching. , 2017, , .		5
455	Reproducible Large-Scale Neuroimaging Studies with the OpenMOLE Workflow Management System. Frontiers in Neuroinformatics, 2017, 11, 21.	2.5	5
456	A Comprehensive Approach for Learning-Based Fully-Automated Inter-slice Motion Correction for Short-Axis Cine Cardiac MR Image Stacks. Lecture Notes in Computer Science, 2018, , 268-276.	1.3	5
457	Volume Change in Frontal Cholinergic Structures After Traumatic Brain Injury and Cognitive Outcome. Frontiers in Neurology, 2020, 11, 832.	2.4	5
458	Multiscale Graph Convolutional Networks for Cardiac Motion Analysis. Lecture Notes in Computer Science, 2021, , 264-272.	1.3	5
459	Going Deeper into Cardiac Motion Analysis to Model Fine Spatio-Temporal Features. Communications in Computer and Information Science, 2020, , 294-306.	0.5	5
460	Unsupervised Cross-domain Image Classification by Distance Metric Guided Feature Alignment. Lecture Notes in Computer Science, 2020, , 146-157.	1.3	5
461	Automated Detection of Congenital Heart Disease in Fetal Ultrasound Screening. Lecture Notes in Computer Science, 2020, , 243-252.	1.3	5
462	Structure Specific Atlas Generation and Its Application to Pancreas Segmentation from Contrasted Abdominal CT Volumes. Lecture Notes in Computer Science, 2016, , 47-56.	1.3	5
463	Fully Convolutional Networks in Medical Imaging: Applications to Image Enhancement and Recognition. Advances in Computer Vision and Pattern Recognition, 2017, , 159-179.	1.3	5
464	Geometric Deep Learning for Post-Menstrual Age Prediction Based on the Neonatal White Matter Cortical Surface. Lecture Notes in Computer Science, 2020, , 174-186.	1.3	5
465	Questionnaires vs Interviews for the Assessment of Global Functional Outcomes After Traumatic Brain Injury. JAMA Network Open, 2021, 4, e2134121.	5.9	5
466	Neurocognitive correlates of probable posttraumatic stress disorder following traumatic brain injury. Brain and Spine, 2022, 2, 100854.	0.1	5
467	The developing brain structural and functional connectome fingerprint. Developmental Cognitive Neuroscience, 2022, 55, 101117.	4.0	5

468 Parameterizing reconfigurable designs for image warping. , 2002, , .

#	Article	IF	CITATIONS
469	3D Statistical Shape Modeling of Long Bones. Lecture Notes in Computer Science, 2006, , 306-314.	1.3	4
470	Coronary artery motion modeling from 3D cardiac CT sequences using template matching and graph search. , 2010, , .		4
471	Improved generation of probabilistic atlases for the expectation maximization classification. , 2011, , .		4
472	Landmark localisation in brain MR images using feature point descriptors based on 3D local self-similarities. , 2012, , .		4
473	Nonrigid free-form registration using landmark-based statistical deformation models. Proceedings of SPIE, 2012, , .	0.8	4
474	Automatic detection of coronary stent struts in intravascular OCT imaging. , 2012, , .		4
475	Fast and accurate global geodesic registrations using knee MRI from the Osteoarthritis Initiative. , 2012, , .		4
476	Automatic segmentation of pediatric brain MRIs using a maximum probability pediatric atlas. , 2012, , .		4
477	Fast Fully Automatic Segmentation of the Severely Abnormal Human Right Ventricle from Cardiovascular Magnetic Resonance Images Using a Multi-Scale 3D Convolutional Neural Network. , 2016, , .		4
478	A Weighted Mirror Descent Algorithm for Nonsmooth Convex Optimization Problem. Journal of Optimization Theory and Applications, 2016, 170, 900-915.	1.5	4
479	Joint Supervoxel Classification Forest for Weakly-Supervised Organ Segmentation. Lecture Notes in Computer Science, 2017, , 79-87.	1.3	4
480	3D FCN Feature Driven Regression Forest-Based Pancreas Localization and Segmentation. Lecture Notes in Computer Science, 2017, , 222-230.	1.3	4
481	Image Guidance for Robotic Minimally Invasive Coronary Artery Bypass. Lecture Notes in Computer Science, 2008, , 202-209.	1.3	4
482	Sample Sufficiency and Number of Modes to Retain in Statistical Shape Modelling. Lecture Notes in Computer Science, 2008, 11, 425-433.	1.3	4
483	Nonrigid Registration and Template Matching for Coronary Motion Modeling from 4D CTA. Lecture Notes in Computer Science, 2010, , 210-221.	1.3	4
484	Coronary Motion Estimation from CTA Using Probability Atlas and Diffeomorphic Registration. Lecture Notes in Computer Science, 2010, , 78-87.	1.3	4
485	A Multi-image Graph Cut Approach for Cardiac Image Segmentation and Uncertainty Estimation. Lecture Notes in Computer Science, 2012, , 178-187.	1.3	4
486	Relating Brain Functional Connectivity to Anatomical Connections: Model Selection. Lecture Notes in Computer Science, 2012, , 178-185.	1.3	4

#	Article	IF	CITATIONS
487	Zen and the art of model adaptation: Low-utility-cost attack mitigations in collaborative machine learning. Proceedings on Privacy Enhancing Technologies, 2022, 2022, 274-290.	2.8	4
488	Extended Coagulation Profiling in Isolated Traumatic Brain Injury: A CENTER-TBI Analysis. Neurocritical Care, 2022, 36, 927-941.	2.4	4
489	Extracting Discriminative Information from Medical Images: A Multivariate Linear Approach. , 2006, , .		3
490	Automatic extraction of the left atrial anatomy from MR for atrial fibrillation ablation. , 2009, , .		3
491	Robust segmentation of brain structures in MRI. , 2009, , .		3
492	4D motion modeling of the coronary arteries from CT images for robotic assisted minimally invasive surgery. Proceedings of SPIE, 2009, , .	0.8	3
493	Landmark detection and coupled patch registration for cardiac motion tracking. Proceedings of SPIE, 2013, , .	0.8	3
494	Consistent and robust 4D whole-brain segmentation: Application to traumatic brain injury. , 2014, , .		3
495	Manifold Learning for Cardiac Modeling and Estimation Framework. Lecture Notes in Computer Science, 2015, , 284-294.	1.3	3
496	Towards Left Ventricular Scar Localisation Using Local Motion Descriptors. Lecture Notes in Computer Science, 2016, , 30-39.	1.3	3
497	Combining Deep Learning and Shape Priors for Bi-Ventricular Segmentation of Volumetric Cardiac Magnetic Resonance Images. Lecture Notes in Computer Science, 2018, , 258-267.	1.3	3
498	Sparse Data–Driven Learning for Effective and Efficient Biomedical Image Segmentation. Annual Review of Biomedical Engineering, 2020, 22, 127-153.	12.3	3
499	Evaluation of the Robustness of Learned MR Image Reconstruction to Systematic Deviations Between Training and Test Data for the Models from the fastMRI Challenge. Lecture Notes in Computer Science, 2021, , 25-34.	1.3	3
500	Improving Phenotype Prediction Using Long-Range Spatio-Temporal Dynamics of Functional Connectivity. Lecture Notes in Computer Science, 2021, , 145-154.	1.3	3
501	Deformation Based Morphometry Analysis of Serial Magnetic Resonance Images of Mouse Brains. Lecture Notes in Computer Science, 2006, , 58-65.	1.3	3
502	Learning-Based Heart Coverage Estimation for Short-Axis Cine Cardiac MR Images. Lecture Notes in Computer Science, 2017, , 73-82.	1.3	3
503	A Framework Combining Multi-sequence MRI for Fully Automated Quantitative Analysis of Cardiac Global And Regional Functions. Lecture Notes in Computer Science, 2011, , 367-374.	1.3	3
504	Real-Time Catheter Extraction from 2D X-Ray Fluoroscopic and 3D Echocardiographic Images for Cardiac Interventions. Lecture Notes in Computer Science, 2013, , 198-206.	1.3	3

#	Article	IF	CITATIONS
505	Prediction of Clinical Information from Cardiac MRI Using Manifold Learning. Lecture Notes in Computer Science, 2015, , 91-98.	1.3	3
506	Representation Disentanglement for Multi-task Learning with Application to Fetal Ultrasound. Lecture Notes in Computer Science, 2019, , 47-55.	1.3	3
507	Transfer Learning for Brain Segmentation: Pre-task Selection and Data Limitations. Communications in Computer and Information Science, 2020, , 118-130.	0.5	3
508	Can We Cluster ICU Treatment Strategies for Traumatic Brain Injury by Hospital Treatment Preferences?. Neurocritical Care, 2021, , 1.	2.4	3
509	Effects of gestational age at birth on perinatal structural brain development in healthy termâ€born babies. Human Brain Mapping, 2022, 43, 1577-1589.	3.6	3
510	Multi-Modal Unsupervised Brain Image Registration Using Edge Maps. , 2022, , .		3
511	Privacy: An Axiomatic Approach. Entropy, 2022, 24, 714.	2.2	3
512	A comparison of the tissue classification and the segmentation propagation techniques in MRI brain image segmentation. , 2005, , .		2
513	Automated localization of periventricular and subcortical white matter lesions. , 2007, , .		2
514	Statistical shape modelling: How many modes should be retained?. , 2008, , .		2
515	Atlas-based registration parameters in segmenting sub-cortical regions from brain MRI-images. , 2009, ,		2
516	Automated quantification and analysis of mandibular asymmetry. , 2010, , .		2
517	Automated quantification and analysis of facial asymmetry in children with arthritis in the temporomandibular joint. , 2011, , .		2
518	Automatic segmentation and identification of solitary pulmonary nodules on follow-up CT scans based on local intensity structure analysis and non-rigid image registration. Proceedings of SPIE, 2011,	0.8	2
519	Localised manifold learning for cardiac image analysis. , 2012, , .		2
520	Hippocampal atrophy in Alzheimer's disease. Neurodegenerative Disease Management, 2012, 2, 197-209.	2.2	2
521	Catheter tracking in 3D echocardiographic sequences based on tracking in 2D X-ray sequences for cardiac catheterization interventions. , 2013, , .		2
522	Multi-scale feature learning on pixels and super-pixels for seminal vesicles MRI segmentation. , 2014, , .		2

#	Article	IF	CITATIONS
523	Automatic quantification of CT images for traumatic brain injury. , 2014, , .		2
524	Discrete Optimisation for Group-Wise Cortical Surface Atlasing. , 2016, , .		2
525	A Multi-resolution Multi-model Method for Coronary Centerline Extraction Based on Minimal Path. Lecture Notes in Computer Science, 2016, , 320-328.	1.3	2
526	CAS-Net: Conditional Atlas Generation and Brain Segmentation for Fetal MRI. Lecture Notes in Computer Science, 2021, , 221-230.	1.3	2
527	Boundary Mapping Through Manifold Learning for Connectivity-Based Cortical Parcellation. Lecture Notes in Computer Science, 2016, , 115-122.	1.3	2
528	A Semi-supervised Large Margin Algorithm for White Matter Hyperintensity Segmentation. Lecture Notes in Computer Science, 2016, , 104-112.	1.3	2
529	Coronary Motion Modelling for Augmented Reality Guidance of Endoscopic Coronary Artery Bypass. Lecture Notes in Computer Science, 2008, , 197-202.	1.3	2
530	Tensor-Based Morphometry of Fibrous Structures with Application to Human Brain White Matter. Lecture Notes in Computer Science, 2009, 12, 466-473.	1.3	2
531	Simultaneous Reconstruction of 4-D Myocardial Motion from Both Tagged and Untagged MR Images Using Nonrigid Image Registration. Lecture Notes in Computer Science, 2010, , 98-107.	1.3	2
532	Flow Analysis in Cardiac Chambers Combining Phase Contrast, 3D Tagged and Cine MRI. Lecture Notes in Computer Science, 2013, , 360-369.	1.3	2
533	Respiratory Motion Correction for 2D Cine Cardiac MR Images using Probabilistic Edge Maps. , 0, , .		2
534	Detecting and Comparing the Onset of Myocardial Activation and Regional Motion Changes in Tagged MR for XMR-Guided RF Ablation. Lecture Notes in Computer Science, 2005, , 348-358.	1.3	2
535	Large Deformation Diffeomorphic Registration Using Fine and Coarse Strategies. Lecture Notes in Computer Science, 2010, , 186-197.	1.3	2
536	Normalisation of Neonatal Brain Network Measures Using Stochastic Approaches. Lecture Notes in Computer Science, 2013, 16, 574-581.	1.3	2
537	Beyond the AHA 17-Segment Model: Motion-Driven Parcellation of the Left Ventricle. Lecture Notes in Computer Science, 2016, , 13-20.	1.3	2
538	Spatial Semantic-Preserving Latent Space Learning for Accelerated DWI Diagnostic Report Generation. Lecture Notes in Computer Science, 2020, , 333-342.	1.3	2
539	Concept of the Munich/Augsburg Consortium Precision in Mental Health for the German Center of Mental Health. Frontiers in Psychiatry, 2022, 13, 815718.	2.6	2
540	<title>Automated camera calibration for image-guided surgery using intensity-based registration</title> ., 2002, 4681, 463.		1

#	Article	IF	CITATIONS
541	Propagating labels of the human brain based on non-rigid MR image registration: an evaluation. , 2005, , .		1
542	Automatic segmentation of brain MRIs and mapping neuroanatomy across the human lifespan. , 2009, , .		1
543	Construction of a dynamic 4D probabilistic atlas for the developing brain. , 2010, , .		1
544	Hippocampal atrophy rate using an expectation maximization classifier with a disease-specific prior. , 2012, , .		1
545	Robust Global Registration through Geodesic Paths on an Empirical Manifold with Knee MRI from the Osteoarthritis Initiative (OAI). Lecture Notes in Computer Science, 2012, , 1-10.	1.3	1
546	Multi-atlas based neointima segmentation in intravascular coronary OCT. , 2013, , .		1
547	Computation on shape manifold for atlas generation: application to whole heart segmentation of cardiac MRI. , 2013, , .		1
548	Improving whole-brain segmentations through incorporating regional image intensity statistics. Proceedings of SPIE, 2013, , .	0.8	1
549	Multi-atlas propagation via a manifold graph on a database of both labeled and unlabeled images. Proceedings of SPIE, 2014, , .	0.8	1
550	Extended boundary shift integral. , 2014, , .		1
551	Artificial Intelligence in Medicine and Privacy Preservation. , 2021, , 1-14.		1
552	Exploring a New Paradigm for the Fetal Anomaly Ultrasound Scan: Artificial Intelligence in Real Time. SSRN Electronic Journal, 0, , .	0.4	1
553	Reducing Textural Bias Improves Robustness of Deep Segmentation Models. Lecture Notes in Computer Science, 2021, , 294-304.	1.3	1
554	Fast Spatio-temporal Free-Form Registration of Cardiac MR Image Sequences. Lecture Notes in Computer Science, 2005, , 414-424.	1.3	1
555	Spectral Clustering as a Diagnostic Tool in Cross-Sectional MR Studies: An Application to Mild Dementia. Lecture Notes in Computer Science, 2008, 11, 442-449.	1.3	1
556	Validation of a Novel Method for the Automatic Segmentation of Left Atrial Scar from Delayed-Enhancement Magnetic Resonance. Lecture Notes in Computer Science, 2012, , 254-262.	1.3	1
557	Differential Dementia Diagnosis on Incomplete Data with Latent Trees. Lecture Notes in Computer Science, 2016, , 44-52.	1.3	1
558	Assessing the Impact of Blood Pressure on Cardiac Function Using Interpretable Biomarkers and Variational Autoencoders. Lecture Notes in Computer Science, 2020, , 22-30.	1.3	1

#	Article	IF	CITATIONS
559	Guest Editorial Special Issue on Mathematical Modeling in Biomedical Image Analysis. IEEE Transactions on Medical Imaging, 2007, 26, 1133-1135.	8.9	0
560	Deformation based morphmetry and atlas based label segmentation: Application to serial mouse brain images. , 2008, , .		0
561	Photo-consistency registration of a 4D cardiac motion model to endoscopic video for image guidance of robotic coronary artery bypass. , 2009, , .		0
562	Reconfigurable acceleration of 3D image registration. , 2009, , .		0
563	Measuring atrophy by simultaneous segmentation of serial MR images using 4-D graph-cuts. , 2010, , .		0
564	A repository of MR morphometry data in Alzheimer's disease and mild cognitive impairment. , 2011, , .		0
565	Exploiting hierarchy in structural brain networks. , 2011, , .		0
566	Incorporating hard constraints into non-rigid registration via nonlinear programming. , 2011, , .		0
567	Motion tracking of left ventricle and coronaries in 4D CTA. , 2011, , .		0
568	Construction of a 4D atlas of the developing brain using non-rigid registration. , 2011, , .		0
569	Data-specific feature point descriptor matching using dictionary learning and graphical models. , 2013, , .		Ο
570	3D cardiac cine reconstruction from free-breathing 2D real-time image acquisitions using iterative motion correction. , 2013, , .		0
571	Fast Deformable Image Registration with Non-smooth Dual Optimization. , 2016, , .		Ο
572	Ageâ€related craniofacial differences based on spatioâ€temporal face image atlases. IET Image Processing, 2019, 13, 1561-1568.	2.5	0
573	Transductive Image Segmentation: Self-training and Effect of Uncertainty Estimation. Lecture Notes in Computer Science, 2021, , 79-89.	1.3	Ο
574	Gradient Projection Learning for Parametric Nonrigid Registration. Lecture Notes in Computer Science, 2012, , 226-233.	1.3	0
575	Automatic Cardiac Motion Tracking Using Both Untagged and 3D Tagged MR Images. Lecture Notes in Computer Science, 2012, , 45-54.	1.3	0
576	Learning Correspondences in Knee MR Images from the Osteoarthritis Initiative. Lecture Notes in Computer Science, 2012, , 218-225.	1.3	0

#	Article	IF	CITATIONS
577	Fast Catheter Tracking in Echocardiographic Sequences for Cardiac Catheterization Interventions. Lecture Notes in Computer Science, 2014, , 171-179.	1.3	0
578	Learning and Combining Image Similarities for Neonatal Brain Population Studies. Lecture Notes in Computer Science, 2015, , 110-117.	1.3	0
579	Learning Optimal Spatial Scales for Cardiac Strain Analysis Using a Motion Atlas. Lecture Notes in Computer Science, 2017, , 57-65.	1.3	0
580	15â€Automatic mis-triggering artefact detection for image quality assessment of cardiac MRI. , 2018, , .		0
581	Flexible Conditional Image Generation of Missing Data with Learned Mental Maps. Lecture Notes in Computer Science, 2019, , 139-150.	1.3	0
582	Artificial Intelligence in Medicine and Privacy Preservation. , 2022, , 145-158.		0